The nuclear monopole Hamiltonian

J. Duflo[1] and A. P. Zuker[2]

[1]*Centre de Spectrométrie Nucléaire et de Spectrométrie de Masse (IN2P3-CNRS), F-91405 Orsay Campus, France*

[2]*IRES, Bâtiment 27, IN2P3-CNRS/Université Louis Pasteur BP 28, F-67037 Strasbourg Cedex 2, France*

(Received 15 December 1997; revised manuscript received 13 November 1998)

The monopole Hamiltonian H_m is defined as the part of the interaction that reproduces the average energies of configurations. After separating the bulk contributions, we propose a minimal form for H_m containing six parameters adjusted to reproduce the spectra of particle and hole states on doubly magic cores. The mechanism of shell formation is then explained. The reliability of the parametrization is checked by showing that the predicted particle-hole gaps are consistent with experimental data, and that the monopole matrix elements obtained provide the phenomenological cure made necessary by the bad saturation and shell properties of the realistic *NN* interaction. Predictions are made for the yet unobserved levels around ^{132}Sn, ^{22}O, ^{34,42}Si, ^{68,78}Ni, and ^{100}Sn and for the particle-hole gaps in these nuclei. [S0556-2813(99)07905-4]

PACS number(s): 21.10.Pc, 21.30.Fe, 21.60.Cs, 27.60.+j

There used to be two kinds of fermion systems: those with many particles and those with few. Nuclei occupied an uneasy middle ground—too large to be studied with the precision of coordinate space methods and too small to take advantage of the simplicity of momentum space—and a new representation had to be invented for them: the harmonic oscillator (HO). As helium droplets and metallic clusters have increased the variety of finite self-bound systems, some typical features of the HO representation may become of general interest, in particular the origin of shell structure, which appears under a new light as a natural by-product of the method we present to circumvent the problem of the bad saturation properties of the potentials derived from *NN* data.

Recent exact results [1,2] for $A \leqslant 8$ indicate that an apparently perfect potential, supplemented by a three-body term produces excellent spectroscopy, but has problems with the absolute binding and symmetry energies and the spin-orbit splittings. Very much the same happens in shell model work, where sophisticated derivations of the effective interaction [3] fail to reproduce the closed shell nature of ^{48}Ca. This problem has been known for a long time, and the solution is simply to readjust some centroids of the interaction [4], defined in terms of the two-body matrix elements as $V_{kl}^{xx'} = \Sigma_J (2J+1) V_{klkl}^{Jxx'} / \Sigma_J (2J+1)$, where xx' stand for neutrons or protons in orbits kl. Much work has gone into deducing these important parameters directly from the data (see, e.g., [5], and references therein), but it was not widely realized (or accepted) that the *only* problem of the realistic interactions is associated with centroids. If these are replaced by fitted ones, the results are excellent [6–8]. Our purpose is to recast the part of the Hamiltonian given in terms of centroids in such a form that it can be deduced directly from experimental data. Therefore, whatever has to be fitted is fitted once and for all, and not case by case.

First we note that matrix elements for a potential of short—but nonzero—range scale as the oscillator frequency $V'(\omega)_{klmn} \cong (\omega/\omega_0) V(\omega_0)_{klmn}$ which is analogous to the inverse-volume scaling in box quantization. (Here, and in what follows, unprimed quantities denote operators stripped of their $\hbar\omega$ factor.) For a realistic *G* matrix, most elements obey quite nicely this ω-scaling law [6,9]. However, it cannot be true for all of them, because then the competition between potential and kinetic energy [which has the same scaling, $K' = \hbar\omega/2\Sigma_p (p+3/2) m_p$, where m_p is the number of particles in HO shell p] would lead to a trivial equilibrium at $\hbar\omega = \infty$ or 0. The terms that cannot scale strictly with ω must be those that go as the total number of particles *A*, since they are alone responsible for saturation. To identify them we separate $H = H_m + H_M$, so that H_m, the monopole Hamiltonian, contains all quadratic (two-body) forms in the scalar products $a_r^+ \cdot a_s$. The full separation is somewhat involved [10], but here we shall need only H_m^d, the diagonal part of H_m—given in terms of the centroids introduced above, and the number operators m_k^x of orbit k in fluid x—a known result,

$$H_m^d = \frac{1}{2} \frac{\hbar\omega}{\hbar\omega_0} \sum_{k,l,x,x'} V_{kl}^{xx'} m_k^x (m_l^{x'} - \delta_{kl}\delta_{xx'}). \qquad (1)$$

A detailed analysis of the realistic interactions shows that the term that goes as A is the collective monopole-monopole force, $W = \Sigma_p (m_p/\sqrt{D_p})^2$, where $D_p = (p+1)(p+2)$ is the degeneracy of HO shell p [11,12]. Therefore, it is here that the $\hbar\omega$ scaling must be supplemented by a more complicated dependence. Now, the combination $\hbar\omega(4K-W)/4$ cancels exactly to order $A^{1/3}$ and (as we shall see) produces strong shell effects: a concrete example of Strutinsky's famous theorem. Therefore we separate it from the rest of the bulk terms, and assume that the saturation mechanism is such that it leads at equilibrium to smooth contributions in A and $A^{2/3}$ and a symmetry energy in $T(T+1)/A$ and $T(T+1)/A^{4/3}$. The part of H_m^d of order $A^{1/3}$ will be called H_m^s hereafter.

Now it is safe(r) to rely on ω scaling and, to force equilibrium conditions, we borrow from [13], $\hbar\omega = 34.6 A^{1/3}/\langle r^2 \rangle = 39/\rho$, where we have used a very accurate fit to the data ($\langle r^2 \rangle = 0.89 \rho A^{1/3}$, a variant of those in [14]), with

$$\rho=[A^{1/3}(1-(2T/A)^2]e^{(3.5/A)}. \tag{2}$$

The factor $1/\rho$ will be tacitly assumed from now on.

The strategy to determine H_m^d follows from the fact that its expectation value for any state is the average energy of the configuration to which it belongs (a configuration is a set of states with fixed m_k^x for each orbit). In particular H_m^d reproduces the exact energy of closed shells (cs) and single particle (or hole) states built on them $[(cs)\pm 1]$, since for this set $(cs\pm 1)$ each configuration contains a single member. As a consequence it is uncontaminated by direct configuration mixing and we have chosen as input data the spectra around doubly magic cores.

Technically, the problem is to recast H_m^d in a form that isolates the few pertinent parameters. The tool [6,10] consists in replacing the set of m_i operators in a major shell by m_p and $\Gamma_{ij}=(m_iD_j-m_jDi)/(D_i+D_j)$, with j arbitrarily chosen. D_i is the degeneracy of orbit (or group of orbits) i. In turn, the m_p could be regrouped to single out the total $m=A$. For the quadratic forms we have (schematically) $m(m-1)$, $(m-1)\Gamma$, and $\Gamma\Gamma$ terms, which behave as constant, one-body, and two-body terms, respectively, for fixed m.

Now we present the operators we (or rather the data) have selected. Two of them behave as one body, $l\cdot s$ and $l\cdot l$, and there are four two-body groups that account for the modifications brought about by the ''intruder'' orbit at the EI (extruder-intruder, i.e., 6,14,28, . . .) closures. To fix ideas, note that the $(cs)\pm 1$ states associated with ^{40}Ca are quite different from those around ^{48}Ca. Their experimental energies are given in the first row of Table I, where the labels of the four two-body groups are also shown: znc, ffc, ffi, and zni. They correspond to the cases in which the intruder and the orbits it acts upon are in the same or different fluids (ff or nz) and the same or different major shells (i or c).

The notation for orbits or groups is p, the full shell; $l=l_>+l_<$, the spin orbit partners, but $q=p_>+p_<$ ($p_>$ is the extruder-intruder orbit, i.e., the largest orbit that migrates to shell $p-1$ to form the EI shell). Then, $R=p-p_>$, $r=p-q$, and finally $\bar{l}=p-l$.

The linear operators are defined through

$$d_p=\sum_l \frac{l+1/2}{p+2}\Gamma_{l_>l_<}, \quad d=l\cdot s=\sum_p d_p, \tag{3a}$$

$$e_p=\sum_l \frac{l(l+1)\Gamma_{l\bar{l}}}{D_p}, \quad e=l\cdot l=\sum_p \frac{p-3}{\sqrt{D_p}}e_p. \tag{3b}$$

There is also a d' operator, identical to d, but restricted to act on r orbits only. Similarly, for e'_p, where now $\bar{l}=r-l$. It can be checked that the $l\cdot l$ displacements are referred to their centroids: $p(p+3)/2$ for e_p and $(p-2)(p+1)/2$ for e'_p. The quadratic operators are given by

$$zncv=\sum_{p\neq p',x\neq y}\frac{\Gamma^x_{p_>R}\Gamma^y_{p'_<r}}{(D_pD_{p'})^{1/4}}, \quad znie=\sum_{p,x\neq y}\frac{m^x_{p>}e^y_p}{D_{p>}}, \tag{4a}$$

$$znie'=\sum_{p,x\neq y}\frac{e'^x_p\Gamma^y_{p_>R}}{D_{p>}}, \quad ffce=\sum_{p\neq p',x}\frac{e^x_pe^x_{p'}}{(D_pD_{p'})^{1/4}}, \tag{4b}$$

$$ffis=\sum_{xp}\frac{m^x_{p_>}}{D_{p_>}}\left(\Gamma^x_{p_>R}-\frac{p(D_p-m^x_p)}{(p+2)(D_p-1)}\right). \tag{4c}$$

There is also a $znid$ operator of the same form as $znie$. The subtraction in $ffis$ ensures that the operator is two body. The denominators are chosen to have splittings of order unity so that they become $O(A^{-1/3})$ when the $1/\rho$ factor is reintroduced.

Using the operators of Eqs. (3) and (4), and the convention of positive binding energies, the combination (coefficients in MeV)

$$\begin{aligned}\rho H^s_m=[&9.53(W-4K+2d+2e)-1.77(2d+2d')\\&+3.63(ffce+2zncv)+7.32ffis\\&+8.35(znie-znie')-2.19znid],\end{aligned} \tag{5}$$

yields a deviation (rms) of 221 keV, in a fit to the (90) experimental $(cs)\pm 1$ energies adopted in Table I. To within 2 keV, the rms deviation is the same for nuclei with $A>60$ and $A<60$.

Figure 1 shows how $W-4K$ produces the HO closures. The coefficient of K, $38/\rho$, which also turns out to be the shell gap, comes spontaneously close to the $\hbar\omega=39/\rho$ estimate. Everything happens as if the naive HO picture were true. The addition of the $l\cdot s$ and $l\cdot l$ terms very much erases the HO closures but *does not produce the EI ones*, which only come about through the action of the two-body terms.

Before inspecting H^s_m in more detail, let us check its reliability through the shell gaps (not included in the fit) given at the bottom of Table I. We have added to H^s_m a symmetry energy $-22[4T(T+1)](1-1.82/\rho)/A$ taken from [12], but reducing the volume term by some 6.5 MeV produced by $W-4K$. At first sight, the agreement with the data [16] seems rather random: the gap in ^{12}C is some 6 MeV too small, in ^{48}Ca it is about perfect, and 1 MeV too large in ^{56}Ni. *But* these are precisely the contributions of the correlation energies coming from accurate shell model work (in [6,7,15], respectively). The omens are good but more calculations are necessary. At the moment Eq. (5) has been tested in the pf shell—where it yields very good spectroscopy [18] and cures the defects of the KB3 interaction [7]—and through Monte Carlo calculations in the full sd-pf shells [17], which cannot provide high precision, but demonstrate its capacity to cope well with very large spaces.

The centroids of $(cs)\pm 1$ spectra are by definition inmune from correlations, but not easy to extract from experiment [19], and the numbers given in Table I are often those of the main peak. In view of uncertainties that may be easily of 300 keV per level, the fit seems to do quite well, and some of the comments that follow, on the individual terms of Eq. (5), are useful in judging the weight to attach to a given prediction.

$d\equiv l\cdot s$. No problem here. The second term is a mild comment.

$e\equiv l\cdot l$ changes sign at $p=3$. This is strange. See next.

TABLE I. Upper boxes: excitation energies. Orbits labeled by $j-1/2p$; so 12 and 2, say, stand for $j=3/2$ and $j=1/2$ in the $p=2$ shell (i.e., $0d_{3/2}$ and $1s_{1/2}$). In the first row of boxes: ground state orbit, element, ZN. In the other rows: orbit, calculated (one decimal) and experimental values (two decimals, parentheses for those not included in the fit). Lower boxes: n gaps $[2\mathrm{BE}(ZN)-\mathrm{BE}(ZN+1)-\mathrm{BE}(ZN-1)]$ and z gaps $[2\mathrm{BE}(ZN)-\mathrm{BE}(Z+1N)-\mathrm{BE}(Z-1N)]$.

12	Ca	**20 19**	33	Ca	**20 21**	2	K	**19 28**	33	Ca	**20 27**	13	Ca	**20 29**	33	Sc	**21 28**
2	1.9	2.40	13	1.9	2.00	12	0.2	0.36	12	2.6	2.58	3	1.9	2.00	13	4.0	4.00
22	6.2	6.00	3	3.8	4.00	22	5.7	5.70	2	3.2	2.60	23	3.9	4.00	3	5.5	5.50
1	13.7		23	5.9	6.00	1	14.2		22	8.6	8.00	44	4.9		23	5.0	4.70
			44	7.5				*znc*			*ffc*	24	8.3	*ffi*	44	8.2	*zni*
1	O	**8 7**	22	O	**8 9**	1	N	**7 14**	22	O	**8 13**	2	O	**8 15**	22	F	**9 14**
11	6.3	6.20	2	0.8	0.87	11	6.7		1	4.1		12	5.7		2	3.1	
0	22.7		12	6.2	6.00	0	27.5		11	10.4		33	7.4		12	5.3	
			33	8.4	8.97							13	10.4		33	9.1	
22	Si	**14 13**	2	Si	**14 15**	22	Al	**13 20**	12	Si	**14 19**	33	Si	**14 21**	2	P	**15 20**
1	4.8	4.20	12	2.0	1.40	1	6.0		2	2.0		13	2.7		12	2.0	2.39
11	10.5		33	5.0	4.00	11	11.8		22	6.7		3	4.8		33	5.6	
			13	8.3					1	13.5		23	5.6		13	8.1	
												44	7.7				
22	Al	**13 28**	33	Si	**14 27**	13	Si	**14 29**	2	P	**15 28**	33	Ni	**28 27**	13	Ni	**28 29**
1	7.5		12	2.3		3	2.1		12	0.1		2	1.7	2.90	23	1.0	0.77
11	13.5		2	3.0		23	3.0		33	4.2		12	3.0	3.60	3	1.4	1.11
			22	9.1		44	4.4		13	10.0		22	8.0		44	3.3	3.50
						24	8.8								24	7.1	
33	Co	**27 40**	3	Ni	**28 39**	44	Ni	**28 41**	13	Cu	**29 40**	33	Co	**27 50**	3	Ni	**28 49**
12	3.5		23	0.4		24	3.0		3	1.3	1.10	2	3.1		44	0.1	
2	4.1		13	1.3		4	4.2		23	1.0	1.21	12	4.9		13	1.4	
22	9.1		33	6.7		34	4.7		44	3.7		22	9.7		23	1.8	
			12	11.3		14	5.3		24	6.9					33	8.1	
						55	6.8										
24	Ni	**28 51**	23	Cu	**29 50**	23	Zr	**40 39**	44	Zr	**40 41**	3	Y	**39 50**	44	Zr	**40 49**
4	1.3		13	1.1		3	0.0		24	2.2		13	1.2	1.51	3	0.4	0.59
34	1.8		3	2.5		13	1.2		4	3.3		23	2.2	1.75	23	2.0	1.45
14	2.4		44	3.3		33	5.6		14	4.4		33	6.8		13	1.6	1.74
55	3.0		24	8.8		12	10.3		34	5.2		12	12.6		33	7.5	
35	7.3								55	6.6							
24	Zr	**40 51**	44	Nb	**41 50**	3	Sn	**50 49**	24	Sn	**50 51**	44	In	**49 82**	14	Sn	**50 81**
4	1.2	1.20	24	4.2		44	1.0		34	0.5		3	0.1	0.35	4	0.3	0.33
14	2.1	2.00	34	4.7		13	1.2		4	0.8		13	1.2		55	0.9	0.24
34	3.0	2.70	4	5.0		23	3.4		14	1.6		23	3.8		24	1.6	1.52
55	3.6		14	5.9		33	7.7		55	2.4		33	7.8		34	2.4	2.43
35	6.9		55	7.4					35	6.1					44	8.2	
35	Sn	**50 83**	34	Sb	**51 82**	4	Tl	**81 126**	5	Pb	**82 125**	46	Pb	**82 127**	45	Bi	**83 126**
45	1.2	(1.56)	24	1.3	0.96	14	0.5	0.35	25	0.5	0.57	56	0.9	0.78	35	1.2	0.90
15	1.3	(0.85)	55	2.7	2.79	55	1.2	1.35	15	0.7	0.90	26	1.2	1.57	66	2.2	1.60
5	2.3	(2.00)	14	2.9	2.71	24	1.9	1.68	66	1.6	1.63	77	1.9	1.42	25	2.6	2.83
66	2.3		4	2.9		34	4.4	4.60	35	2.1	2.34	6	2.0	2.03	15	2.9	3.12
25	2.4		35	7.8		44	7.9		45	3.0	3.41	36	2.3	2.49	5	3.6	3.60
46	6.1								55	8.2		16	2.6	2.54	46	7.0	
												57	5.3				
	C	**6 6**		C	**6 8**		O	**8 8**		O	**8 14**		O	**8 20**		Si	**14 4**
n gap	7.9	13.78	*n* gap	4.7	6.96	*n* gap	6.5	11.52	*n* gap	4.0	4.11	*n* gap	2.9		*n* gap	7.1	8.71
z gap	7.9	14.01	*z* gap	7.1	10.62	*z* gap	6.5	11.53	*z* gap	6.5	9.99	*z* gap	10.5		*z* gap	7.1	8.84
	Si	**14 20**		Si	**14 28**		Ca	**20 20**		Ca	**20 28**		Ni	**28 28**		Ni	**28 40**
n gap	3.8	5.06	*n* gap	6.1		*n* gap	5.2	7.28	*n* gap	4.8	4.80	*n* gap	7.4	6.39	*n* gap	2.8	2.85
z gap	6.1	6.55	*z* gap	7.7		*z* gap	5.2	7.24	*z* gap	4.9	6.18	*z* gap	7.4	6.47	*z* gap	6.4	5.91
	Ni	**28 50**		Zr	**40 40**		Zr	**40 50**		Sn	**50 50**		Sn	**50 82**		Pb	**82 126**
n gap	5.7		*n* gap	3.7		*n* gap	4.7	4.77	*n* gap	6.0		*n* gap	4.3	4.89	*n* gap	3.0	3.43
z gap	6.5		*z* gap	3.7		*z* gap	1.8	2.00	*z* gap	6.0		*z* gap	5.5	6.07	*z* gap	3.5	4.20

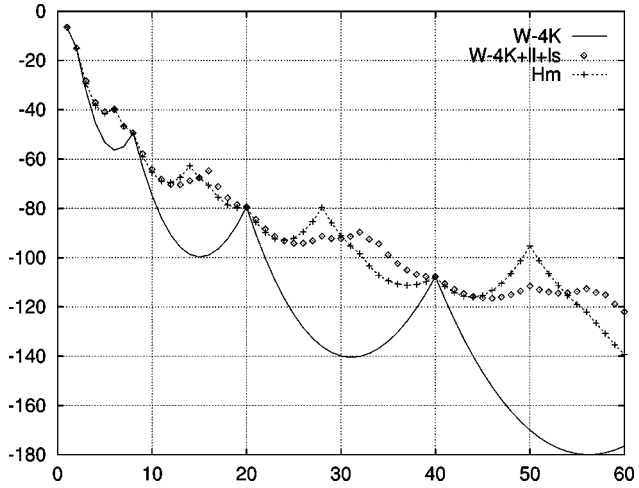

FIG. 1. Monopole shell effects in the binding energies of $T=0$ nuclei.

$ffce+2zncv$. The $2s_{1/2}$ orbit is the great troublemaker: responsible for halos, for the change in sign in $l\cdot l$, it also comes too low in ^{47}Ca, about right in ^{47}K and too high in ^{55}Ni. There is no possible monopole combination that can place the three levels at their observed positions; only correlations can do it. [By analogy we expect in $A=99$ a smaller observed splitting between 3 ($p_{1/2}$) and 44 ($g_{9/2}$) than in Table I.] However, the overall action of the term is very sound. In particular $zncv$ does very well for the recently observed 13-23 ($p_{3/2}$-$f_{5/2}$) splittings [20]: 0.53 MeV in ^{71}Cu and 0.17 MeV in ^{73}Cu, calculated at 0.5 and 0.1 MeV, respectively. The same comment applies to the evolution of 24-34 splittings in Sb.

$ffis$ by itself turns ^{48}Ca into a closed shell. *It is this term that the realistic interactions conspicuously fail to produce.* It is a good test for the proposed three-body potentials.

$zni\ldots$. This is a complicated mixture that the realistic interactions seem to reproduce reasonably, although some repulsion between the $p_>$ and R orbits is missing (same effect as for $ffis$, but weaker). This term needs revisiting, but its effects are quite sound; in particular, they reproduce the radical change of spectra between ^{48}Ca and ^{56}Ni.

The correspondence between $(cs)\pm 1$ j levels around ^{133}Sn and $j+1$ levels around ^{209}Pb is striking, and the calculations strictly respect the experimental orderings, except for the intruder ($p_>$) orbits, which are known to be the most affected [21] by particle-vibration coupling. The predicted sequence in ^{133}Sn shows an inversion with respect to the (somewhat speculative) experimental assignment [22].

The $W-4K$ operator that initializes the shell formation mechanism should be common to self-bound systems. The way the HO closures evolve into the observed ones then depends on specifics, but the nuclear example could serve as a modeling guide.

A preliminary version of this work was completed during the stay of A.Z. at the Institute for Nuclear Theory at the University of Washington, whose hospitality and excellent working conditions are thankfully acknowleged.

[1] B. S. Pudliner, V. R. Pandharipande, J. Carlson, S. Pieper, and R. W. Wiringa, Phys. Rev. C **56**, 1720 (1997).
[2] R. W. Wiringa, in Proceedings of the 15th International Conference on Few Body Problems, Groningen, 1997 (unpublished).
[3] M. Hjorth-Jensen, T. T. S. Kuo, and E. Osnes, Phys. Rep. **261**, 125 (1995).
[4] E. Pasquini, Ph.D. thesis, Report No. CRN/PT 76-14, Strasburg, 1976; E. Pasquini and A. P. Zuker, in *Physics of Medium Light Nuclei*, Florence, 1977, edited by P. Blasi and R. Ricci (Editrice Compositrice, Bologna, 1978).
[5] S. Pittel *et al.*, Phys. Rev. C **48**, 1050 (1993).
[6] A. Abzouzi, E. Caurier, and A. P. Zuker, Phys. Rev. Lett. **66**, 1134 (1991).
[7] G. Martínez-Pinedo, A. P. Zuker, A. Poves, and E. Caurier, Phys. Rev. C **55**, 187 (1997).
[8] A. P. Zuker, in *Contemporary Shell Model*, edited by X. W. Pan, Springer Lecture Notes in Physics Vol. 482 (Springer, New York, 1997).
[9] G. Bozzolo, A. Klar, and J. P. Vary, Phys. Rev. C **29**, 1069 (1984).
[10] A. P. Zuker, Nucl. Phys. **A576**, 65 (1994).
[11] M. Dufour and A. P. Zuker, Phys. Rev. C **54**, 1641 (1996).
[12] J. Duflo and A. P. Zuker, Phys. Rev. C **52**, R23 (1995).
[13] A. Bohr and B. Mottelson, *Nuclear Structure* (Benjamin, Reading, MA, 1964), Vol. I.
[14] J. Duflo, Nucl. Phys. **A576**, 29 (1994).
[15] E. Caurier, G. Martínez-Pinedo, A. Poves, and A. P. Zuker, Phys. Rev. C **52**, R1736 (1995).
[16] G. Audi and A. H. Wapstra, Nucl. Phys. **A565**, 1 (1993).
[17] D. Dean *et al.*, Phys. Rev. C (submitted).
[18] F. Nowacki (private communication).
[19] Electronic version of Nuclear Data Sheets, http://www.dne.bnl.gov/nndc.html
[20] S. Francho *et al.*, Phys. Rev. Lett. **81**, 3100 (1998).
[21] I. Hamamoto, Phys. Rep., Phys. Lett. **10C**, 63 (1974).
[22] P. Hoff *et al.*, Phys. Rev. Lett. **77**, 1020 (1996).